RESEARCH ARTICLE

Atmospheric precursors for intense summer rainfall over the United Kingdom

Richard P. Allan[1] 🔵 | Stephen Blenkinsop[2] | Hayley J. Fowler[2] |
Adrian J. Champion[3]

[1]National Centre for Earth Observation, Department of Meteorology, University of Reading, Reading, United Kingdom

[2]School of Engineering, Newcastle University, Newcastle, United Kingdom

[3]College of Engineering, Mathematical and Physical Sciences, University of Exeter, Exeter, United Kingdom

Correspondence
Richard P. Allan, Department of Meteorology, Whiteknights, University of Reading, Reading, United Kingdom.
Email: r.p.allan@reading.ac.uk

Abstract

Intense sub-daily summer rainfall is linked to flooding impacts in the United Kingdom. Characterizing the atmospheric conditions prior to the rainfall event can improve understanding of the large-scale mechanisms involved. The most intense sub-daily rainfall intensity data generated from rain gauge records across the United Kingdom over the period 1979–2014 are combined with fields from the ERA Interim reanalysis to characterize atmospheric conditions prior to heavy rainfall events. The 200 most intense 3-hourly events for six UK regions are associated with negative anomalies in sea level pressure (<-2 hPa) and 200 hPa geopotential height (<-60 m) to the west or south west of the United Kingdom 1 day earlier, with above average moisture, evaporation and dew point temperature over North West Europe. Atmospheric precursors are more intense but less coherent between regions for composites formed of the 25 heaviest rainfall events but all display substantial moisture transport from the south or south east prior to their occurrence. Composites for the heaviest events are characterized by a tripole geopotential anomaly pattern across the North Atlantic. Above average geopotential height and dew point temperature over Newfoundland and below average geopotential height but elevated evaporation in the North Atlantic are found to be weakly associated with an increased chance of the most intense sub-daily rainfall events 5–9 days later.

KEYWORDS
Europe, extreme precipitation, hydrological cycle, observations, Reanalyses, water vapour

1 | INTRODUCTION

Flash flooding from intense rainfall can lead to loss of life and severe damage to infrastructure and the environment (Hapuarachchi *et al.*, 2011; Flack *et al.*, 2019). There is not a simple link between precipitation and flooding (Stephens *et al.*, 2015; Wasko and Sharma, 2017). However, flood events are often caused by sustained, heavy precipitation culminating in river flooding as well as intense sub-daily rainfall which can lead to flash flooding in urban environments and small river catchments (Smith and Ward, 1998). The intensity of rainfall is expected to increase as atmospheric moisture, and its transport into storms, amplifies with a warming climate (Allan *et al.*, 2014; Fischer and Knutti, 2016; Pfahl *et al.*, 2017). Although intensity increases close to those expected for low level water vapour ($\sim 7\%$/K) are physically reasonable, the exact magnitude of change is uncertain, depending upon timescale and spatial extent as well as less well understood dynamical and microphysical factors (Blenkinsop *et al.*,

2015; O'Gorman, 2015; Pendergrass *et al.*, 2016; Bao *et al.*, 2017; Lenderink and Fowler, 2017; Ali *et al.*, 2018; Guerreiro *et al.*, 2018; Nie *et al.*, 2018; Pendergrass, 2018).

In mid-latitude regions, flooding events have been linked with atmospheric rivers (Dettinger *et al.*, 2011; Lavers *et al.*, 2011; Gimeno *et al.*, 2014; Lavers *et al.*, 2016): linear synoptic features of exceptional water vapour transport within mid-latitude cyclones (Dacre *et al.*, 2014, 2019). Although this link appears robust for the winter half year, atmospheric precursors to extreme daily rainfall in the United Kingdom are distinct in summer months (Allan *et al.*, 2015) with atmospheric rivers not playing an important role (Champion *et al.*, 2015). The increased importance of smaller-scale systems such as thunderstorms during summer motivates a separate assessment of this season where convection within frontal rain bands and mesoscale convective systems also play a role in surface water flooding and rapid water rise within small river catchments (Carlson and Ludlam, 1968; McGinnigle, 2002; Golding *et al.*, 2005; Lewis and Gray, 2010). Since these processes are operating at smaller scales than can be explicitly represented even by higher spatial resolution numerical simulations (Kendon *et al.*, 2014; Chan *et al.*, 2016), this motivates the assessment of the large-scale atmospheric processes that are important for the generation of intense sub-daily rainfall.

Champion *et al.* (2019) characterized atmospheric conditions prior to intense sub-daily rainfall in summer over two UK regions estimated from a compilation of quality controlled, hourly rain gauge data (Blenkinsop *et al.*, 2016). Here we investigate in more detail the regional-scale precursors to intense sub-daily rainfall, extending to all UK regions and exploiting the latest, updated quality controlled rain gauge data (Blenkinsop *et al.*, 2016; Lewis *et al.*, 2018). Complimenting Champion *et al.* (2019). Here we focus on synoptic precursors in the west Europe region as well as the large-scale North Atlantic, considering additional thermodynamic variables, including evaporation and dew point temperature, which display stronger links with extreme precipitation changes than surface air temperature (Lenderink and van Meijgaard, 2010). While Champion *et al.*

(2019) also considered atmospheric stability metrics (e.g., wet bulb potential temperature), which are physically linked with intense thunderstorms and mesoscale convective systems (Lewis and Gray, 2010), in the present study we are interested primarily in the larger scale precursors relating to atmospheric circulation patterns and moisture amount and transport.

2 | DATA AND METHODS

2.1 | 3-hourly rainfall observations

A quality-controlled, hourly rainfall dataset was developed by Blenkinsop *et al.* (2016) using available automated rain gauges across the United Kingdom. Here we employ an update to this dataset that implemented additional quality checks on an extended record and removed stations containing inconsistencies with a gridded daily product (Lewis *et al.*, 2018). A peaks-over-threshold (POT) method was applied to extract the highest intensity events for gauge locations across the United Kingdom, considering events during the summer months (June–August), the time of year in which the most extreme events are concentrated (Gray and Marshall, 1998; Darwish *et al.*, 2018). A POT3 sample was used whereby three events per complete year of data are extracted for each station. For example, a gauge record comprising 20 years of data would yield the 60 (3 × 20) largest events in the record. This ensures that extreme events occurring in the same year are not missed, as could be the case when using annual maxima, while limiting to three events to avoid biasing estimates to a single station or year. Consistent with Champion *et al.* (2019), we consider 3-hourly aggregates of rainfall observations which are thought to relate to flash flooding to a greater extent than hourly intensities.

The locations of the gauges are displayed in Figure 1, highlighting the heaviest 25 and 200 rainfall events across the United Kingdom, along with the ranked
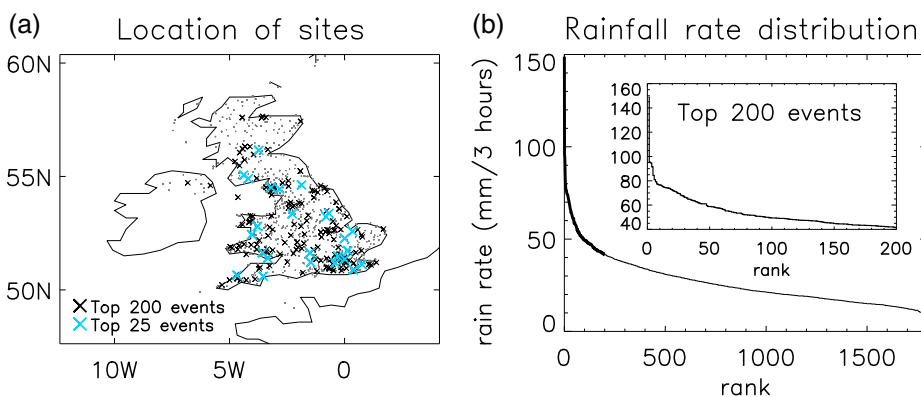
FIGURE 1 (a) Geographical location of 3-hr summer rainfall events (left) including location of heaviest 200 and 25 rainfall events (other events are marked as dots). (b) The ranked rain rate across all events (the heaviest 200 events in the inset) [Colour figure can be viewed at wileyonlinelibrary.com]

3-hour rain rate across all unique events from the POT3 sample (with the top 200 events in the inset). Of the 29,929 summer POT3 events, 1,773 events are retained when removing duplicate days. This represents about half of the total number of summer days between 1979 and 2014 (3,312), confirming that many events are not extreme and motivating analysis of the heaviest events. The heaviest 200 events identified in each of six UK regions are analysed with details of the heaviest five events in each region listed in Table 1. The regions split the United Kingdom up into six geographical areas, illustrated in Figure 2 (region names are defined in Table 1). A region-specific perspective is beneficial since the nature of extremes depends upon location and geography. Although a more objective approach to selecting regions would account more fully for extreme rainfall behaviour (Jones *et al.*, 2013), the objective here is to seek atmospheric precursors rather than analysing extreme characteristics so the approach adopted is deemed adequate for the purposes of the present study.

2.2 | Additional quality control checks

The heaviest 3-hr rainfall totals that passed prior quality control checks were first cross-referenced with Met Office

TABLE 1 Ranked heaviest 3-hourly rainfall events (ending on the hour indicated) for summer months (June–August) across six UK regions 1979–2014 (see Figure 2: West Scotland and Northern Ireland [including Isle of Man], WSNI; East Scotland, ES; Northwest England and Wales, NWEW; eastern England, EE; Southwest England and Wales, SWEW; Southeast England, SEE)

Region/rank	Location	Lat	Lon	Altitude (m)	Date	hr	Rain (mm)
WSNI/1	Upper Black Laggan	55.06	−4.39	411	August 20, 1989	19	91.5
WSNI/2	Low Creoch	54.90	−4.19	17	June 6, 2010	16	75.6
WSNI/3	Dingwall	57.60	−4.45	10	June 29, 2004	13	66.2
WSNI/4	Dingwall	57.60	−4.45	10	August 12, 1988	19	54.8
WSNI/5	Ronaldsway	54.08	−4.63	17	July 26, 1985	20	53.4
ES/1	Tillicoultry	56.15	−3.73	30	July 26, 2004	07	76.8
ES/2	Whitley Bay	55.05	−1.45	15	June 28, 2012	18	58.6
ES/3	Hatton	57.43	−1.91	40	August 23, 2010	18	56.4
ES/4	Kinloss	57.65	−3.56	6	July 11, 1982	03	50.3
ES/5	Monaughty/Black Burn	57.61	−3.42	55	August 25, 2008	11	49.2
NWEW/1	Rhydymain/Cae'r-defaid	52.80	−3.79	361	July 3, 2001	18	148.8
NWEW/2	Honister	54.51	−3.20	360	August 24, 2005	06	84.4
NWEW/3	Kentmere	54.44	−2.83	261	July 5, 2006	20	81.0
NWEW/4	Bow Street	52.44	−4.03	16	July 18, 2006	10	75.0
NWEW/5	Ringway	53.36	−2.28	70	August 6, 1981	03	73.0
EE/1	Uttons Drove	52.27	0.00	15	August 8, 2014	17	94.7
EE/2	High Marnham	53.23	−0.81	19	August 9, 2004	20	77.4
EE/3	Copley	54.62	−1.87	257	July 1, 2009	17	76.6
EE/4	Upton/Sturgate Airfield	53.37	−0.68	13	June 22, 1982	21	74.0
EE/5	Denver Sluice	52.58	0.35	0	July 28, 2005	15	71.0
SWEW/1	Ashcombe	50.60	−3.53	102	August 5, 2012	13	74.5
SWEW/2	Rhoose/Cardiff Airport	51.40	−3.34	65	August 2, 1995	17	74.3
SWEW/3	Slaughterbridge	50.64	−4.67	212	August 16, 2004	15	72.5
SWEW/4	Mynydd Werfa	51.64	−3.57	567	August 24, 1987	10	71.3
SWEW/5	Bodrane	50.43	−4.53	128	August 11, 2004	23	67.4
SEE/1	Andover	51.22	−1.47	63	August 6, 2009	11	95.4
SEE/2	Thornwood	51.72	0.14	76	June 10, 1993	20	79.2
SEE/3	Bethersden	51.13	0.75	35	June 27, 1994	11	76.4
SEE/4	Holmbury	51.19	−0.41	155	July 15, 2008	01	74.2
SEE/5	Kew Gardens	51.48	−0.29	5	July 6, 1983	16	73.7
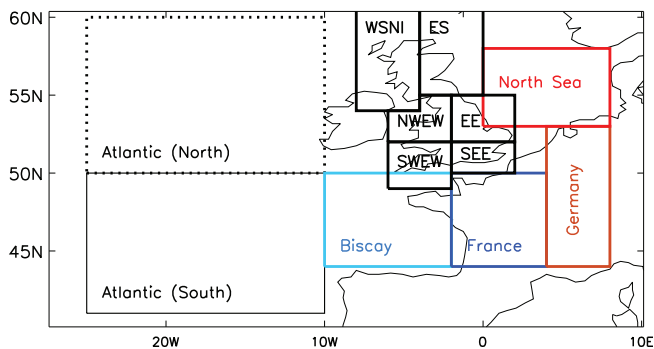
FIGURE 2 Location of regions for UK rainfall events detailed in Table 1 and remote regions considered for atmospheric precursor timeseries analysis [Colour figure can be viewed at wileyonlinelibrary.com]

daily weather summaries[1] and manually checked against nearby gauges. Spurious events can occasionally be recorded when gauges become blocked and then subsequently discharge the accumulated water. This was assessed for the heaviest events by comparing rainfall totals with accumulations over multiple days at nearby sites. For example, events recorded at Boreland (ES 20/8/2009, 61.5 mm) and Llanfyrnach (SWEW 11/8/2008, 89.6 mm) were identified as accumulations and removed. Sustained spurious behaviour compared with nearby sites was also identified at Portmoak (August 2007) and Meadowfoot/Wanlockhead (4/8/2000, 82 mm), both in the ES region, motivating their removal.

There is a fine balance between screening out unreliable totals and removing genuine but highly localized events that do not appear in nearby gauges. Further work is still required to develop an optimal, objective methodology that uses minimal manual intervention to retain a robust record of intense sub-daily rainfall. Nevertheless, the pragmatic approach employed here proved useful in identifying suspect events in an earlier version of the dataset which were independently identified and removed from the updated version of the quality controlled rainfall dataset used in the present analysis. For example, events recorded at two low altitude south east England sites (104.8 mm on the 15th August at Radlett and 100 mm at Mogden/Isleworth in west London on July 23, 2012) and the Higher Hill upland (451 m) site (NWEW 28/8/1990, 140 mm) were removed by the updated quality control following Lewis *et al.* (2018) and the additional manual checks. These events were included in the composites of Champion *et al.* (2019) (their Table 1). Preliminary analysis had also marked these events as suspect based on a lack of corroborating evidence from the Met Office daily weather reports and the Mogden observations during the 17:25 and 17:49

event were marked as *unchecked* in the raw data. Similarly, events recording above 70 mm on the 13th and 25th July at Pant Mawr (an upland NWEW station) were also removed by the updated quality control as were many events recording above 100 mm of rainfall for stations in south Wales including Cowbridge, Nantyrwdd and Sennybridge.

2.3 | ERA interim reanalysis data

Atmospheric conditions prior to the 3-hourly rainfall extremes (atmospheric precursors) were extracted from the European Centre for Medium-range Weather Forecasts (ECMWF) Interim reanalysis (ERA Interim), a state of the art reanalysis system covering the period 1979-present (Dee *et al.*, 2011). A fixed configuration of the ECMWF atmospheric model was observationally constrained using 4-dimensional data assimilation. We considered $0.75 \times 0.75°$ latitude/longitude resolution 6-hourly data, extracting dew point temperature (Td), pressure at mean sea level ($PMSL$), surface evaporation (E), geopotential height at 200 hPa ($Z200$), column-integrated water vapour (CWV) and column integrated horizontal water vapour transport (WVT) calculated from the eastward and northward components as:

$$WVT = \sqrt{\left(\frac{1}{g}\int_{p_s}^{0} qudp\right)^2 + \left(\frac{1}{g}\int_{p_s}^{0} qvdp\right)^2}, \quad (1)$$

where g is acceleration due to gravity, p is atmospheric pressure, p_s is surface pressure, q is specific humidity, u is eastward wind and v is northward wind. CWV and WVT are useful measures of total atmospheric water vapour and its horizontal transport that have previously been linked with heavy rainfall events (Lavers *et al.*, 2011; Gimeno *et al.*, 2014).

2.4 | Evaluation of heaviest rainfall events

Following the additional quality control checks, each extreme 3-hr duration summer rainfall event was matched with the daily mean atmospheric conditions using the variables extracted from ERA Interim on the days leading up to the event. Anomalies were subsequently computed by subtracting the pentad climatology centred on the calendar day and these were formed into composites across 25 or 200 of the most intense rainfall events up to 9 days prior to each event. The region 30°W–10°E, 40–60°N is assessed in detail with a wider North Atlantic region also considered.

Where multiple events occurred in a single day the heaviest event was retained (Section 2.1) for each of the regions considered (WSNI, ES, NWEW, EE, SWEW, SEE; defined in Table 1). For all POT3 events, 37% of WSNI events were retained while for the remaining regions between 10% (SEE, EE) and 23% (ES) of daily events were retained. This makes sense as in the more sparsely gauged and geographically complex WSNI and ES regions, each rainfall event or associated events affect fewer separate sites. In other regions, synoptic events leading to heavy rainfall are often large-scale in nature and affect multiple gauging sites, particularly where in close proximity. Removing events occurring on the same day ensures that atmospheric precursors associated with events affecting multiple gauges in a single day are not given extra weight when composites are computed over multiple events (i.e., the events are independent).

To illustrate the method, Figure 3 displays atmospheric conditions the day before the heaviest event in each region (which are geographically depicted by boxes in the right column). Since the recorded intensity occurs at different times of day, the lead time will differ somewhat but keeping to calendar day is preferred for simplicity. Of the most intense events listed in Table 1, the NWEW region contains the heaviest 3-hr rainfall total (148 *mm*). The heaviest three events for this region were all recorded for altitudes of at least 260 m. Although altitude clearly plays a role in determining rainfall intensity of some sites, there is a range of station altitudes for the top five events across regions. Contrasting intensities across the regions motivates a regional analysis of atmospheric precursors.

There is a diverse range of synoptic precursors to the heaviest 3-hourly events recorded in each region (Figure 3). Most events are associated with cyclonic flows and low geopotential to the north or north west of the United Kingdom, the exception being for the Tillicoultry event (Figure 3d–f). There is not a consistent signal for dew point temperature or evaporation although there are some indications of high evaporation rates over continental Europe. Although atmospheric river patterns were not found to be a driver of extreme daily rainfall in summer (Champion *et al.*, 2015), linear moisture transport features are present for some of the heaviest 3-hourly rainfall events, for example in the NWEW region (Honister, Bow Street and Ringway) and the WSNI region including the Black Laggan and both Dingwall events (not shown).

Most of the heaviest events that were scrutinized are clearly identified in the Met Office daily summaries (see endnote 1). The Black Laggan event (Figure 3a–c) matches reports of thunderstorms in southern Scotland associated with an advancing cold front. The fifth heaviest WSNI event at Ronaldsway also matches a reported

thunderstorm associated with high dew point temperature and a cyclonic southeasterly flow that led to 47 mm of rainfall in 2 hr. The heaviest rainfall event observed (Rhydymain; Figure 3g–i) coincides with reports of heavy and thundery showers with localized downpours over western Britain associated with a convergence line ahead of a cold front; this also generated an area of thundery showers that moved north over northern Wales during the evening, probably associated with a mesoscale convective system as part of a "modified" Spanish Plume synoptic pattern (Lewis and Gray, 2010). Other events in the NWEW region appear consistent with reports of heavy rain in the daily weather summaries and the Ringway event on the sixth August 1981 coincides with mesoscale convective systems (Gray and Marshall, 1998). The Uttons Drove EE event (Figure 3j–l) is clearly associated with some very heavy, thundery downpours that developed over central England associated with a developing low pressure moving from the south.

For the SWEW region, torrential downpours on the fifth August 2012, associated with slow moving showers that resulted in localized flooding,[2] match the SWEW Ashcombe event and the Rhoose/Cardiff Airport event is corroborated by reports of thunderstorms widely affecting southern Britain (Institute of Hydrology, 1996). The Slaughterbridge event is associated with the same intense convergence line that generated the Boscastle flood of 2004. For SEE, the Andover event on the sixth August 2009 (Figure 3p–r) is corroborated by reports of a line of heavy and thundery showers extending from the Isle of Wight to Lincolnshire associated with a static cold front and rainfall rates exceeding 10 mm·hr^{-1} were recorded at Heathrow (see endnote 1). The Thornwood event also matches reports of flooding in the national media and evidence of mesoscale convective systems (Gray and Marshall, 1998). Thunderstorms reported in the Met Office daily summaries corroborate the Kew event on the sixth July 1983, yet totals at nearby Heathrow were only 18 mm over the same 3-hr period, indicative of the localized nature of thunderstorms, though inaccuracies in the extreme totals cannot be ruled out.

Some cases, while appearing plausible in relation to the synoptic patterns and often associated with weather fronts, could not be clearly identified as a heavy rainfall event. Although quality control removed many of the heaviest ES events, of the remaining records, the Tillicoultry event (Figure 3d–f) remains suspect despite no clear signs of spurious gauge behaviour as does the Kinloss ES observation (July 11, 1982) that could only be matched with a mesoscale convective system that was far to the south (Gray and Marshall, 1998).

The lack of confirmation of some events in independent records highlights the continuing importance of
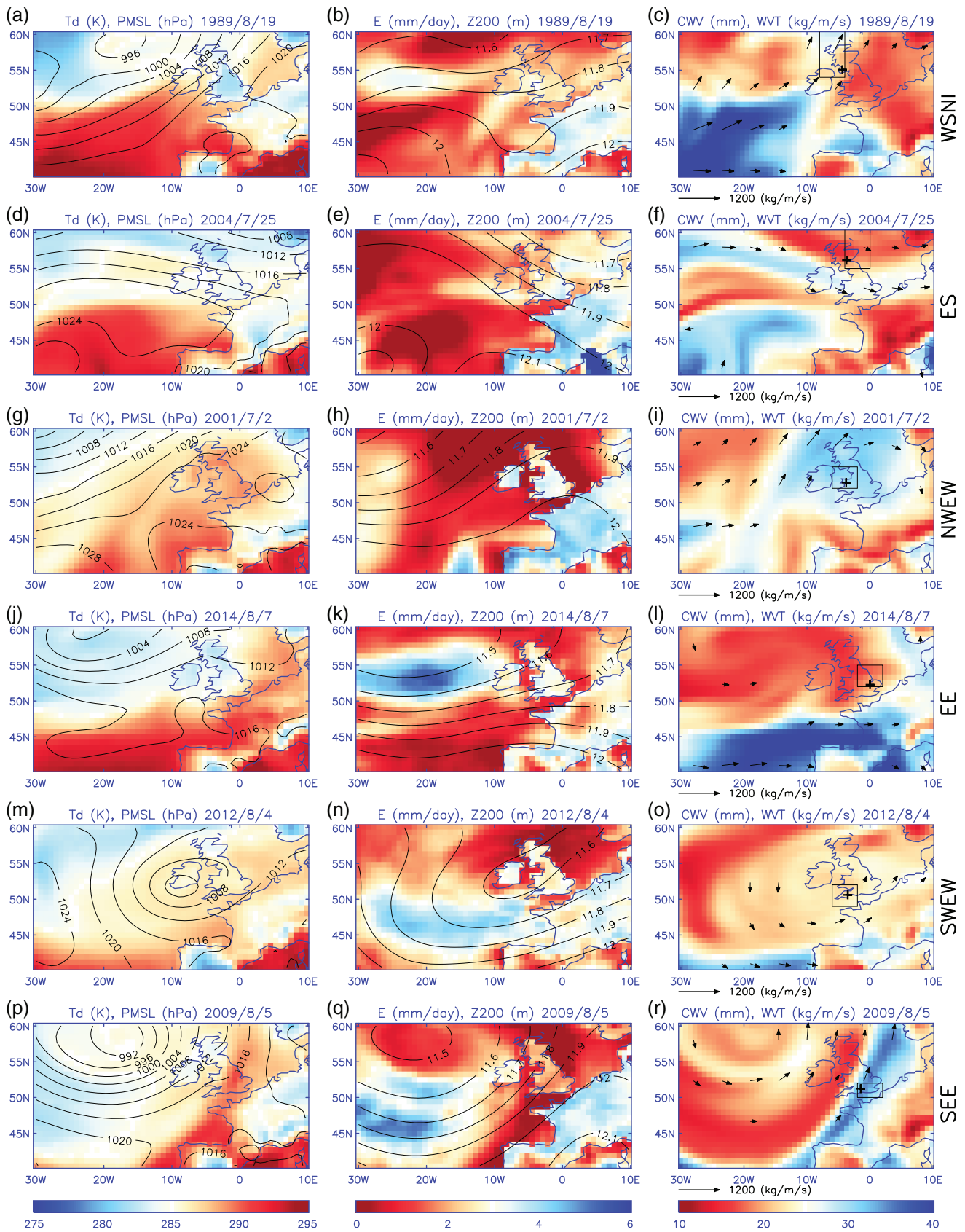
FIGURE 3 Atmospheric conditions on the day before the single heaviest recorded 3-hourly summer rainfall event in each of six UK regions (denoted by boxes in right column with gauge location marked as +). Left column: dew point temperature (*Td*, colours) and pressure at mean sea level (*PMSL*, contours). Middle column: Evaporation (*E*, colours) and geopotential height at 200 hPa (*Z200*, contours). Right column: Column integrated water vapour (*CWV*, colours) with arrows denoting water vapour transport magnitude and direction (*WVT*) [Colour figure can be viewed at wileyonlinelibrary.com]

consistency checking across datasets and further questions the timing, magnitudes or existence of some of the events despite careful quality control (Blenkinsop *et al.*, 2016; Lewis *et al.*, 2018). This also motivates the use of composites of atmospheric precursors across a number of heavy rainfall events.

3 | COMPOSITES OF ATMOSPHERIC PRECURSORS TO SUB-DAILY RAINFALL EXTREMES

3.1 | Atmospheric precursors 1-day prior to intense rainfall events

Daily-mean synoptic conditions 1-day prior to the day of the heaviest 25 or 200 3-hourly rainfall events within each of the six regions were extracted from the ERA Interim reanalysis. Anomalies were computed relative to the pentad-mean climatology centred on each date and composites formed for each variable considered (Figures 4 and 5). Stippling denotes where anomalies in Td, E and CWV are significantly different from zero at the 90% confidence level based upon a two-tailed t test (e.g., Lavers *et al.*, 2015), assuming $n - 1$ degrees of freedom, where n is the number of events in the composite.

One day prior to the heaviest 200 events in each region, negative pressure anomalies (around -2 to -4 hPa) and geopotential anomalies (around -60 to -100 m) are present to the west or south west of the United Kingdom (Figure 4). This is consistent with an anomalous cyclonic southerly airflow and associated moisture transport from the south affecting the United Kingdom, with elevated dew point temperature and moisture across North West Europe and elevated evaporation in continental North West Europe but also to the west of the United Kingdom over the Atlantic associated with cool, relatively dry northerly winds. Anomalously low ocean evaporation to the south east of France ($4°E$, $43°N$), apparent for all event composites, is presumably explained by occasionally very high evaporation rates associated with the hot, dry summer form of the Mistral wind that is inhibited during the southerly flows associated with intense summer rainfall in the United Kingdom. Interestingly, the suspect Tillicoultry event displays an opposite sign of evaporation anomaly in this region (Figure 3e) relating to a northerly airflow associated with a Mediterranean cyclone to the east.

Precursor composites for the heaviest 25 events (Figure 5) display more diversity across regions and generally larger magnitude anomalies in atmospheric fields compared to the 200 event composite (Figure 4). As with

the 200 member composite, the heaviest 25 events are associated with above average evaporation to the west of the United Kingdom and over continental Europe with positive Td and CWV anomalies over Western Europe and anomalously strong integrated moisture transport from the south west, south and south east. There is similarity in anomaly patterns for the ES, EE and SWEW regions with strong cyclonic southerly flow and negative anomalies in $PMSL$ (<-2 hPa) and $Z200$ (<-100 m) to the south west of the United Kingdom. A contrasting orientation of the geopotential height anomaly field for SEE and NWEW (Figure 5h,q) is associated with moisture transport from the south east (Figure 5i,r).

Precursors to intense daily rainfall were previously found to be distinct in summer months compared to other seasons for south east England (Allan *et al.*, 2015). Nevertheless, the importance of higher moisture amount and transport in determining these heavy rainfall events is consistent with previous analysis of daily events and underlines how thermodynamic increases in moisture in a warming climate are anticipated to intensify precipitation extremes (Fischer and Knutti, 2016; Lenderink and Fowler, 2017).

3.2 | Time dependence of precursors to intense rainfall events

The emergence over time of the large-scale atmospheric precursors to intense summer rainfall is useful in understanding the mechanisms involved and in seeking linkages between large-scale weather patterns many days before the events. The time dependence of precursors to the heaviest events in the south east England (SEE) and North West England/Wales (NWEW) regions are now described.

Positive geopotential height anomalies over the United Kingdom are apparent 4 days prior to the south east England events (Figure 6b) symptomatic of weakly anticyclonic conditions. High evaporation rates over North West Europe and the Atlantic Azores region emerge 2 days before the event (Figure 6e). Time series of atmospheric precursors averaged over ocean and land regions surrounding the United Kingdom (illustrated in Figure 2) up to 9 days prior to the rainfall events are also analysed. There are increases in moisture ($\sim$3–4 mm; Figure 7a) and dew point temperature ($\sim$1 K; Figure 7d) from 4 days prior to the events over France, Germany, the North Sea and over the local SEE region. Surface pressure and geopotential height also drop during this period over SEE and France/Biscay (Figure 7b,c) with elevated evaporation over Germany and the Atlantic south region. Moisture transport increases from 6 days
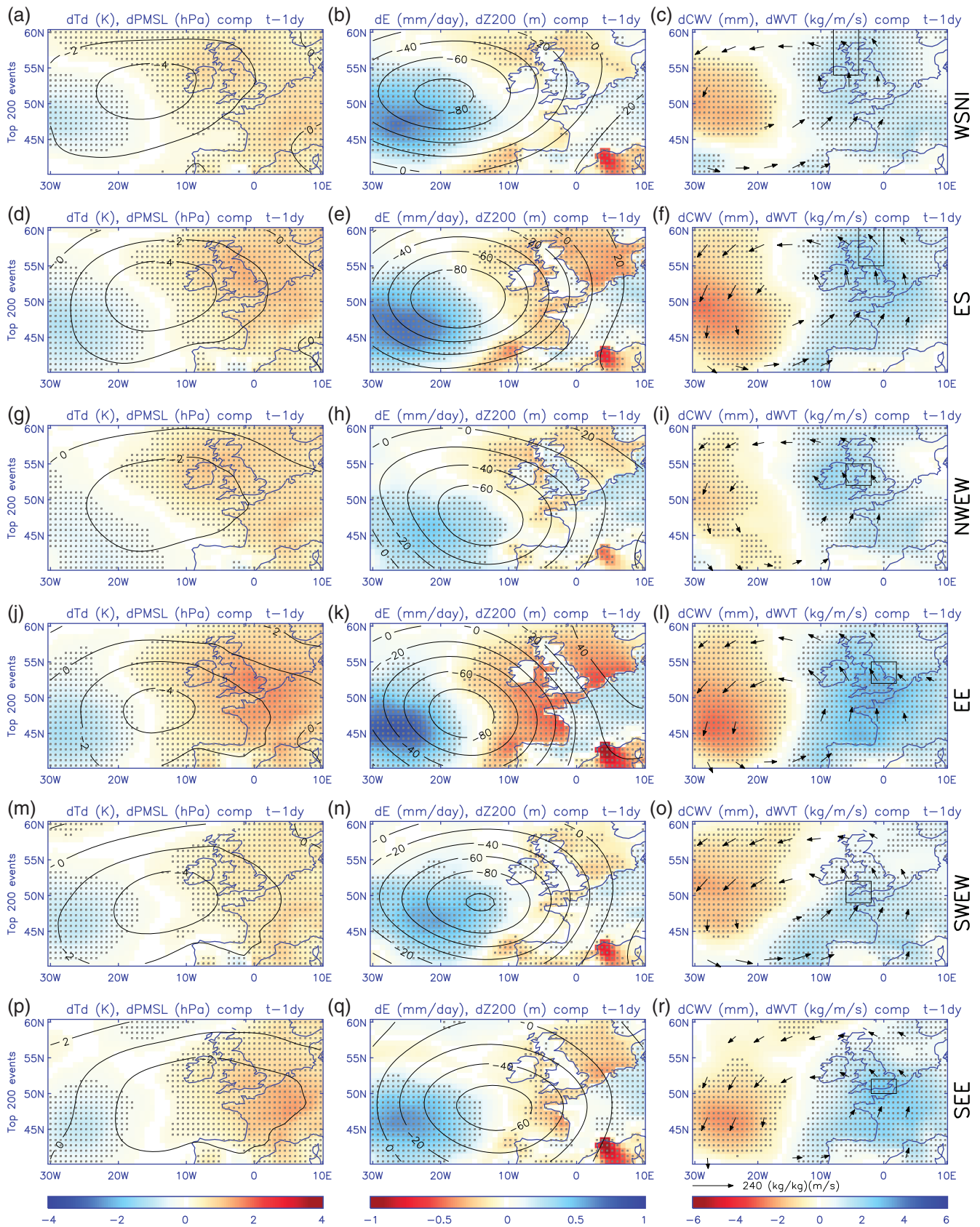
FIGURE 4 Atmospheric precursor composites of anomalies 1-day prior to the 200 heaviest regional 3-hourly summer rainfall events for the WSNI (a–c), ES (d–f), NWEW (g–i), EE (j–l), SWEW (m–o) and SEE (p–r) regions defined in Table 1. Left column: dew point temperature (*Td*, colours) and pressure at mean sea level (*PMSL*, contours). Middle column: Evaporation (*E*, colours) and geopotential height at 200 hPa (*Z200*, contours). Right column: Column integrated water vapour (*CWV*, colours) with arrows denoting water vapour transport (*WVT*). Stippling denotes where anomalies in *Td*, *E* and *CWV* are significantly different from zero at the 90% confidence level [Colour figure can be viewed at wileyonlinelibrary.com]
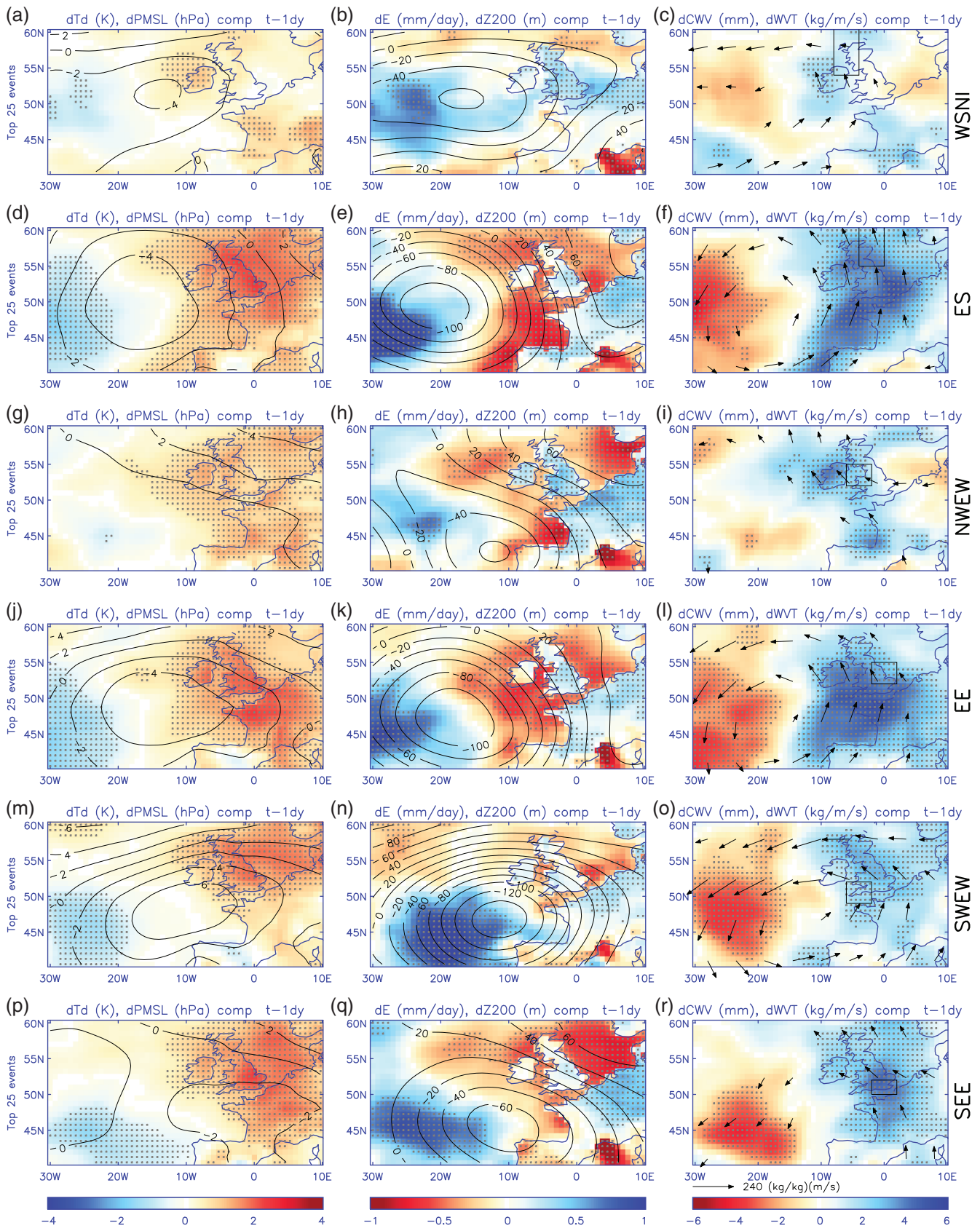
FIGURE 5 As Figure 4 but for composites of the 25 heaviest regional 3-hourly summer rainfall events [Colour figure can be viewed at wileyonlinelibrary.com]
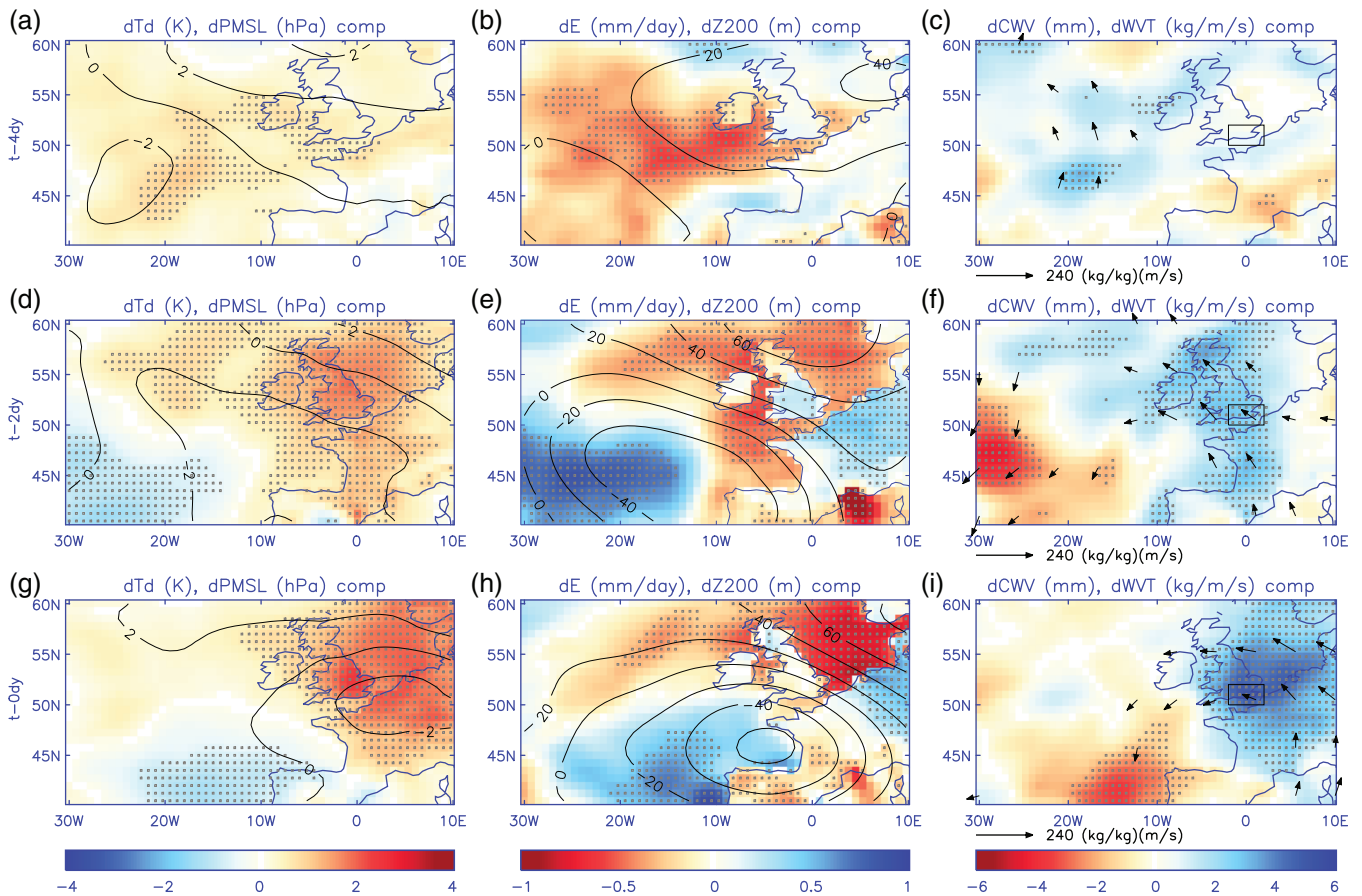
FIGURE 6 Atmospheric precursor composites (a–c) 4 days, (d–f) 2 days and (g–i) on the day of the 25 heaviest regional 3-hourly summer rainfall events for South East England (SEE). Left column: dew point temperature (*Td*, colours) and pressure at mean sea level (*PMSL*, contours). Middle column: Evaporation (*E*, colours) and geopotential height at 200 hPa (*Z200*, contours). Right column: Column integrated water vapour (*CWV*, colours) with arrows denoting water vapour transport (*WVT*) [Colour figure can be viewed at wileyonlinelibrary.com]

prior to the event in SEE and over the North Sea from 3 days prior, primarily due to an enhanced east to west component (Figure 7f–h).

For the heaviest 200 events affecting SEE (Figure 8), moisture and dew point temperature increase in the local SEE region by a similar magnitude to the 25-event composite but with increases more gradually from 7 days prior to the events with less variance across the composite as denoted by the shading (Figure 8a,d). Decreases in geopotential height (∼4 hPa) and sea level pressure (∼40 m) affect the SEE region from 2 to 3 days prior to the events and also the Biscay region where evaporation increases are also most pronounced. Increases in moisture transport from 8 days prior to the event are most pronounced over the North Sea region (60 kg·m^{-1}·s^{-1}) but in contrast to the more extreme 25-member composite this is dominated by enhanced northward vapour transport from 4 days prior that also affects the France/Germany/SEE regions. Positive geopotential height anomalies affect the North Sea for south east and eastern

England events (SEE/EE) which are symptomatic of a weak anticylonic influence.

In general water vapour transport increases over most regions considered in the days prior to the 200 composite events (Figure 8h) while the signal of anomalous southward transport in Atlantic regions to the west of the United Kingdom and enhanced northward transport for regions to the south and east of the United Kingdom (Figure 8g) are associated with cyclonic conditions centred to the west of the United Kingdom. Negative anomalies in geopotential height (<−40 m) and high evaporation rates to the west of the United Kingdom and positive moisture and dew point temperature anomalies over the United Kingdom are present in the 200 event composite 4 days prior (Figure 9), though the dynamical signals are weak for the SEE region. This could reflect contrasting dynamical factors explaining intense sub-daily rainfall events over south eastern England (Allan *et al.*, 2015) although elevated dew point temperature and moisture appear robust.
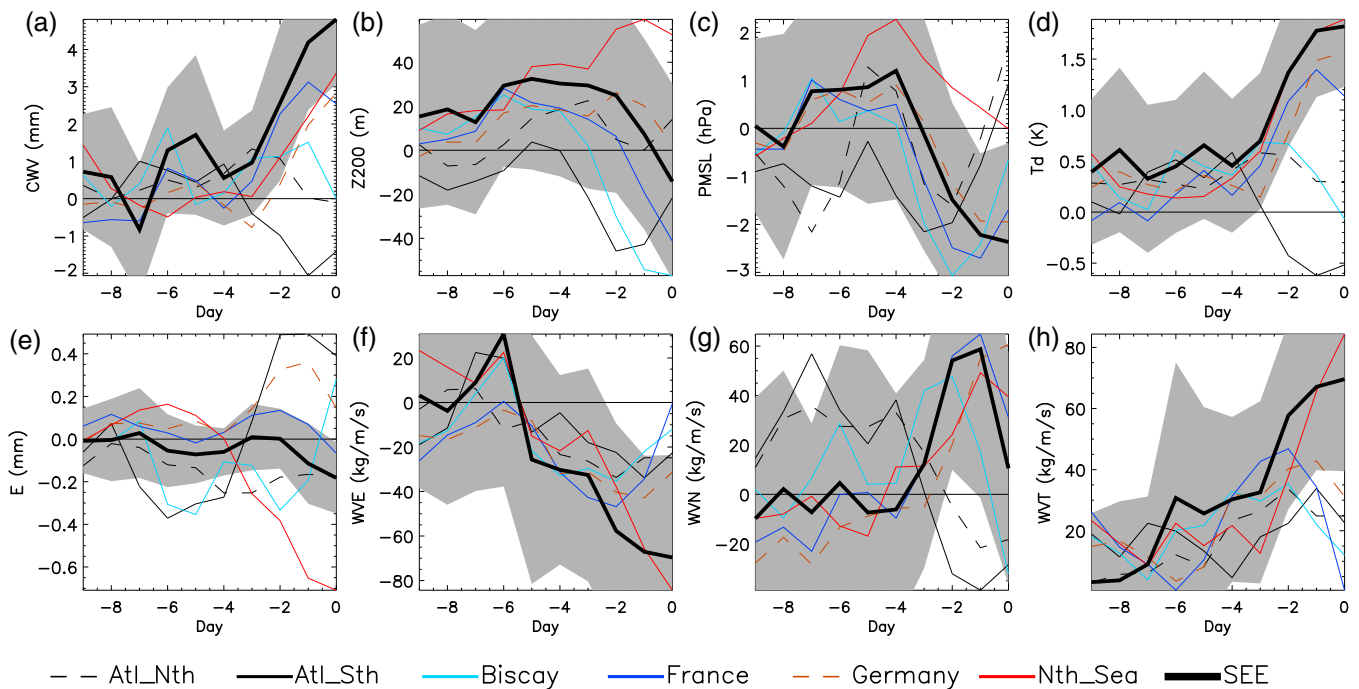
FIGURE 7 Regional anomaly mean composites of atmospheric variables (averaged over the 7 regions surrounding the UK depicted in Figure 2) prior to the heaviest 25 3-hourly rainfall events over South East England (SEE) 1980–2014: (a) column integrated water vapour (mm), (b) geopotential height at 200 m, (c) pressure at mean sea level (hPa), (d) dew point temperature (K), (e) evaporation (mm·day^{-1}), (f) eastward water vapour transport (kg·m^{-1}·s^{-1}), (g) northward water vapour transport (kg·m^{-1}·s^{-1}) and (h) magnitude of water vapour transport (kg·m^{-1}·s^{-1}). The grey shaded region represents ±1 standard deviation across the 25 events making up the composite for the region local to the event [Colour figure can be viewed at wileyonlinelibrary.com]
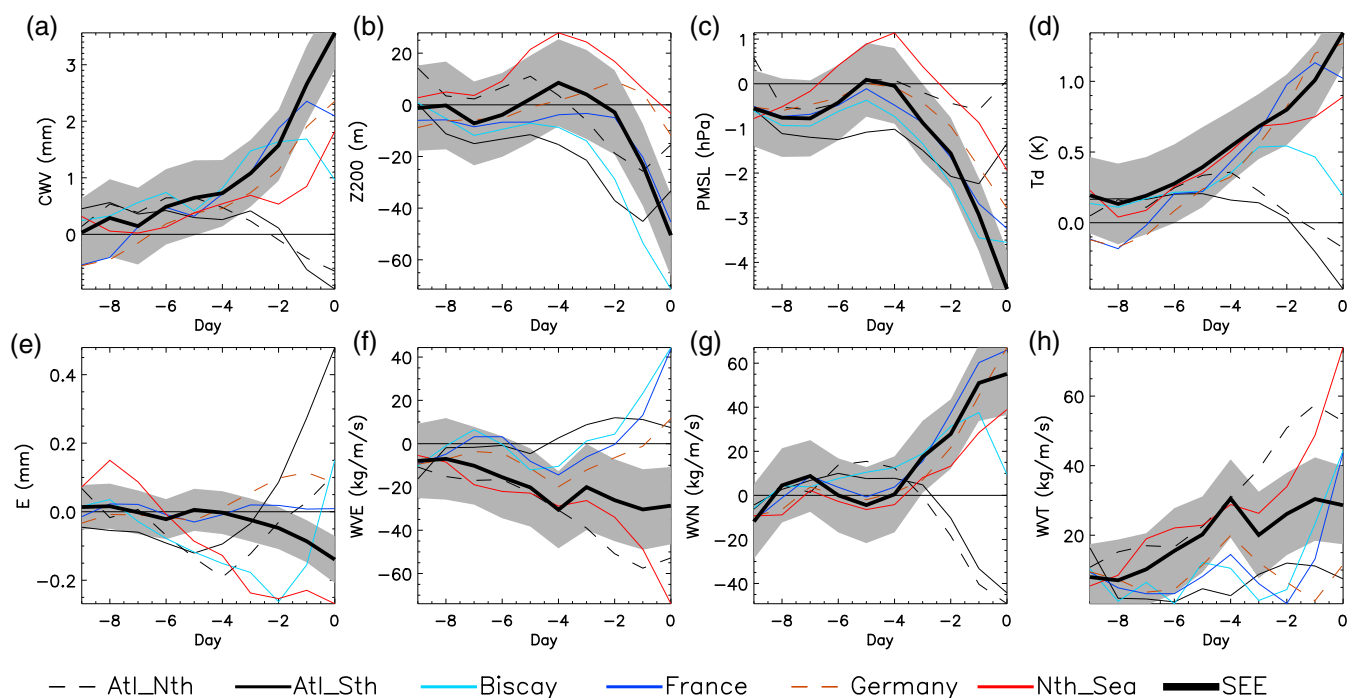
FIGURE 8 As Figure 7 but for time dependence of atmospheric precursors prior to the heaviest 200 SEE events [Colour figure can be viewed at wileyonlinelibrary.com]
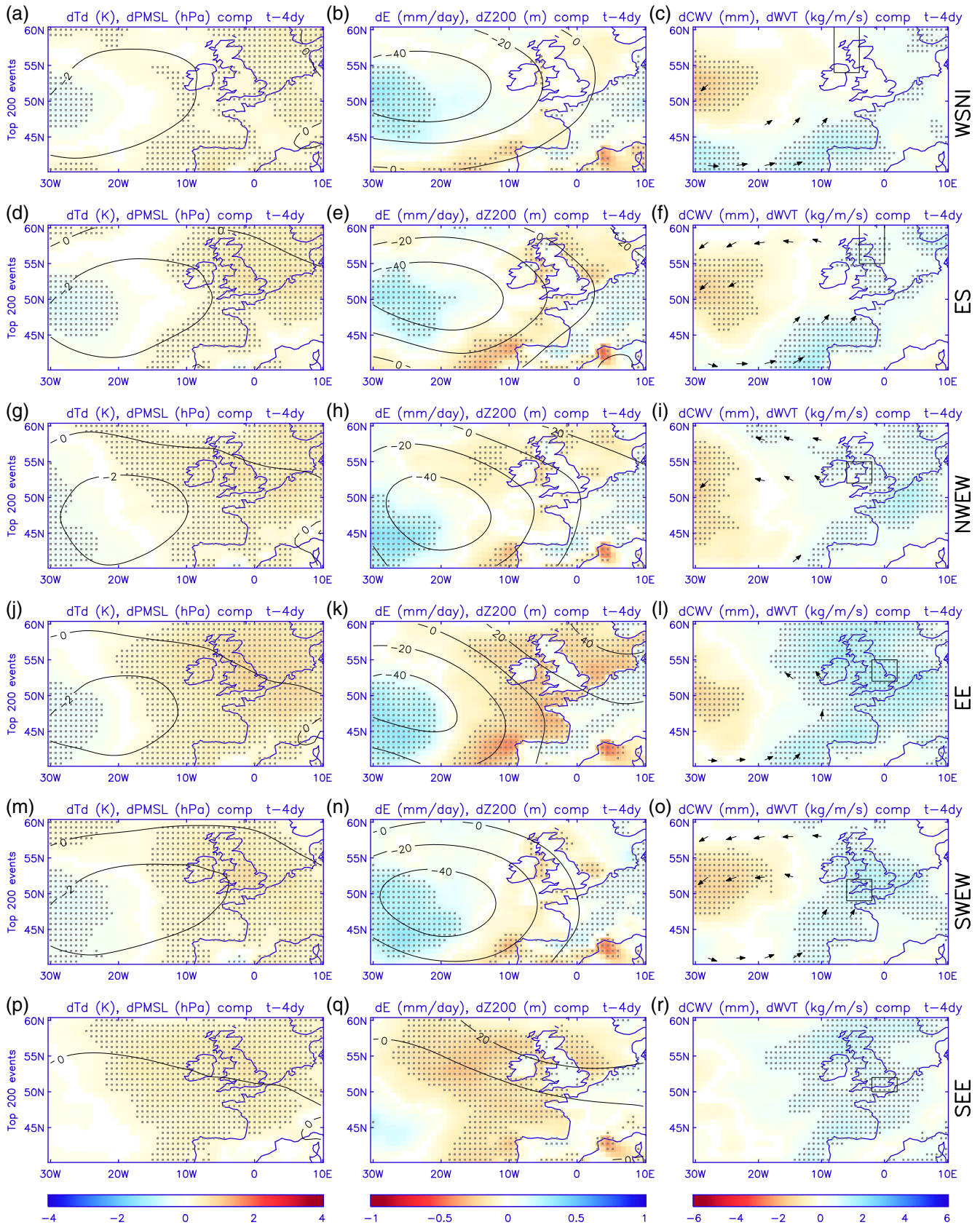
FIGURE 9   As Figure 4 but for atmospheric precursors 4 days prior to heaviest 200 events across all UK regions [Colour figure can be viewed at wileyonlinelibrary.com]

Over north western England and Wales (NWEW), the day of the most intense 3-hourly rainfall events are characterized by high dew point temperature, moisture and moisture transport from the south east over the United Kingdom region with elevated evaporation over much of north western continental Europe (Figure 10g–i), consistent with analysis of daily rainfall extremes (Allan *et al.*, 2015). This is associated with a dipole of negative sea level pressure and geopotential anomalies to the south west of the United Kingdom and positive anomalies to the north east (Figure 10g,h), which are present but weaker at 2 and 4 days prior to the events and shifted to the west (Figure 10d,e and a,b). The signal of anomalously strong moisture transport from the south is also shifted to the west of the United Kingdom 4 days prior to the events (Figure 10c) indicating that a slow, eastward propagation of large-scale weather patterns precede the intense rainfall events.

Time series up to 9 days prior to the events for the NWEW region display consistent increases in moisture and its northward transport (Figure 11). In the 2 days prior to the rainfall events, moisture transport is high in the regions to the south and east of the United Kingdom (Biscay/France/Germany; Figure 11h). Anomalously

high geopotential height 4 days prior to rainfall events (>40 m) are present over the Germany/North Sea/NWEW regions (Figure 7b), suggesting weakly anticyclonic conditions that are also associated with low moisture over the United Kingdom (Figure 10c). Negative geopotential height anomalies over the Atlantic to the west 4 days prior move to the south west of the United Kingdom leading up to the event. Given the robust signal in geopotential height anomalies across the North West Europe region affecting all regions 1–4 days prior to the events (Figures 4–10), a larger spatial scale perspective, as also considered by Champion *et al.* (2019), is therefore deemed necessary to understand the atmospheric context for these anomalies.

3.3 | Atmospheric precursors at the North Atlantic scale

Previous work has found blocking of the jet stream over the North Atlantic to influence thunderstorm activity over Europe (Mohr *et al.*, 2019) through promoting or inhibiting the advection of warm, moist and unstable air masses from the south or southwest. This will depend on
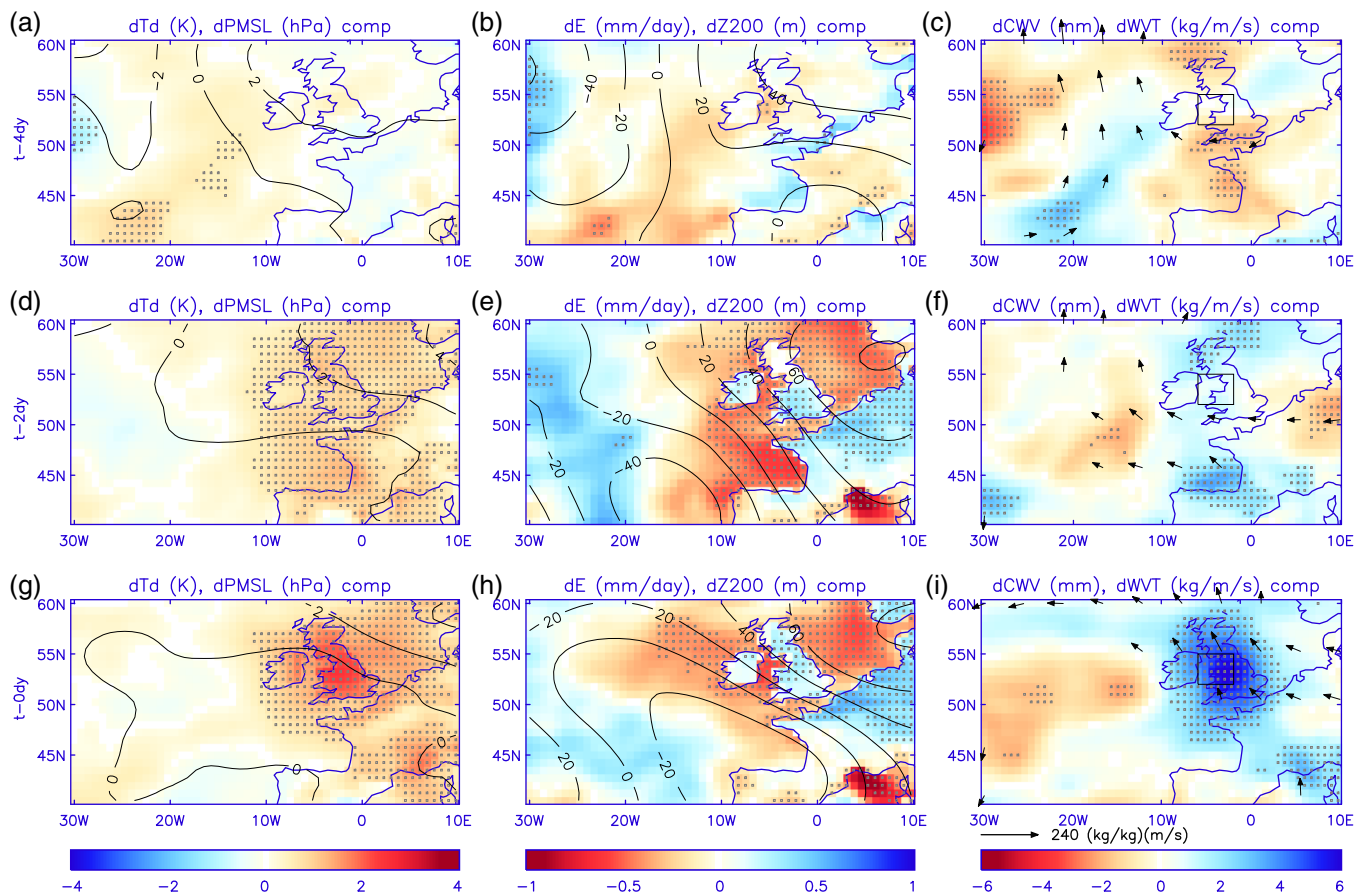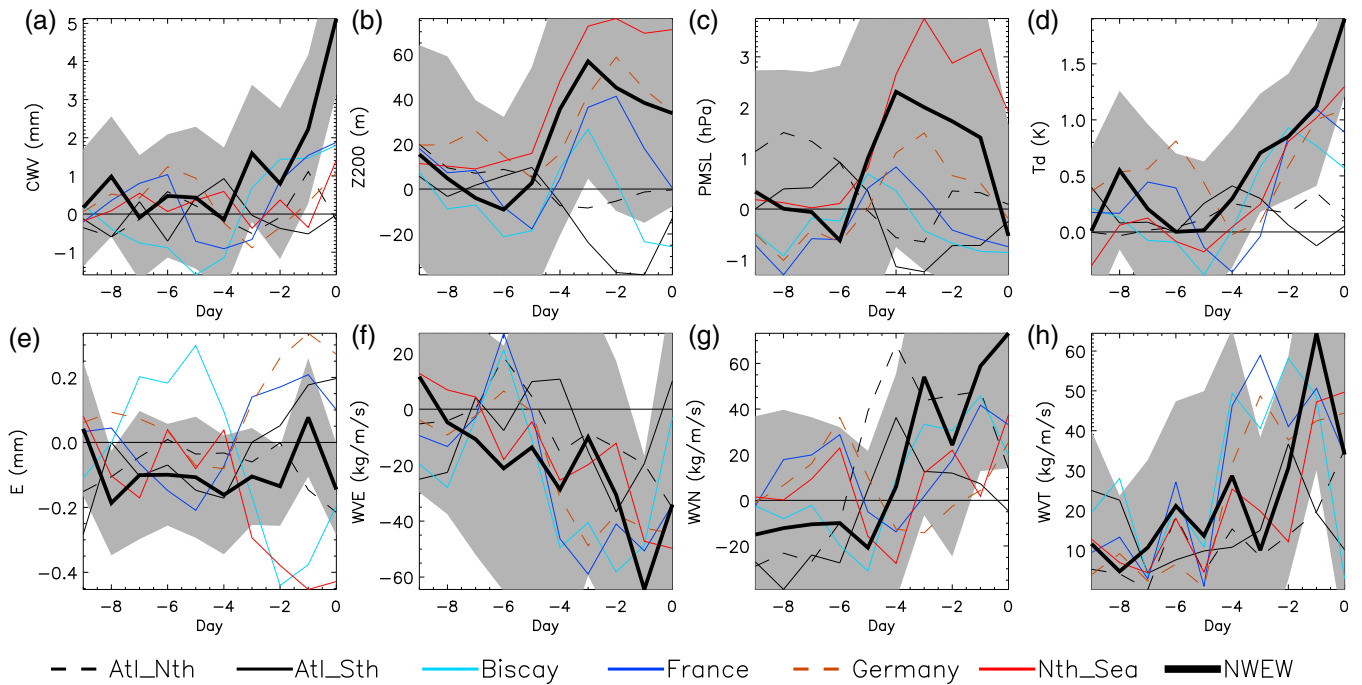

FIGURE 10 As Figure 6 but for NW England and N Wales (NWEW) [Colour figure can be viewed at wileyonlinelibrary.com]

FIGURE 11 Regional anomaly mean composites of atmospheric variables prior to the heaviest 25 3-hourly rainfall events, as Figure 7 but over North West England and North Wales (NWEW) [Colour figure can be viewed at wileyonlinelibrary.com]

the location of the block in relation to the region of suppressed or enhanced activity. We therefore now consider the larger-scale precursors to the summer sub-daily rainfall extremes in three UK regions.

Composites of the large-scale atmospheric precursors to the heaviest 25 rainfall events for the WSNI, NWEW and SEE regions were computed across the larger North Atlantic region to assess the more remote influences. Atmospheric fields 5 days prior to the heaviest 3-hr events are displayed in Figure 12. Consistent with Champion *et al.* (2019), the geopotential height fields display coherent patterns with some weak signals of high evaporation rates in the North West Atlantic and strong moisture fluxes affecting parts of the North Atlantic, particularly for WSNI precursors. Elevated dew points are seen over Newfoundland from 9 days prior to the events with increasing evaporation in the mid North Atlantic from 5 days prior, with both signals propagating towards the east (not shown). The geopotential height fields are characterized by a tri-pole pattern with elevated values over Newfoundland (NFL) and near the United Kingdom with depressed values in the central northern Atlantic (CNA) around 40–50°W, 50–60°N (see boxes in Figure 12b).

The tripole pattern of geopotential height appears to signify a meandering jet stream that, for the cases identified, promotes a warm, moist flow towards the United Kingdom from the south. Francis and Vavrus (2015) use geopotential height contours and the ratio of meridional and zonal wind components to diagnose the waviness of

the jet stream and its changes over time; here we focus on the geopotential height anomalies linked with the identified heavy rainfall events and as such are not able to make a simple link to the jet stream structure.

Guided by the results in Figure 12, to investigate the role of the geopotential height field in intense summer rainfall, an index (Z_I) was constructed to take a ratio of the NFL (60–70°W, 40–50°N) and CNA (30–50°W, 50–60°N) anomalies averaged over the boxes displayed in Figure 12b,e:

$$Z_I = \frac{Z200_{NFL}}{Z200_{CNA}}. \qquad (2)$$

For WSNI we alter the regions due to the shifted anomaly field (NFL: 60–70°W, 50–60°N; CNA: 20–40°W, 50–60°N).

When applying the SEE/NWEW index to the whole United Kingdom, 12 of the 25 heaviest 3-hourly rainfall events (48%) were preceded by the highest 20% of Z_I anomalies 9 days prior to the events (not shown), consistent with the composites previously constructed. However, only 1.8% of the highest 20% of Z_I anomalies match any of the heaviest 25 events 9 days later. Although this is more than double the probability due to chance (25 events out of 3,312 total days = 0.7%) this does not seem to suggest the metric is a useful predictor of heavy rainfall events. Similar results are obtained for the 25 most intense events in the NWEW region (Table 2) while there is less correspondence for
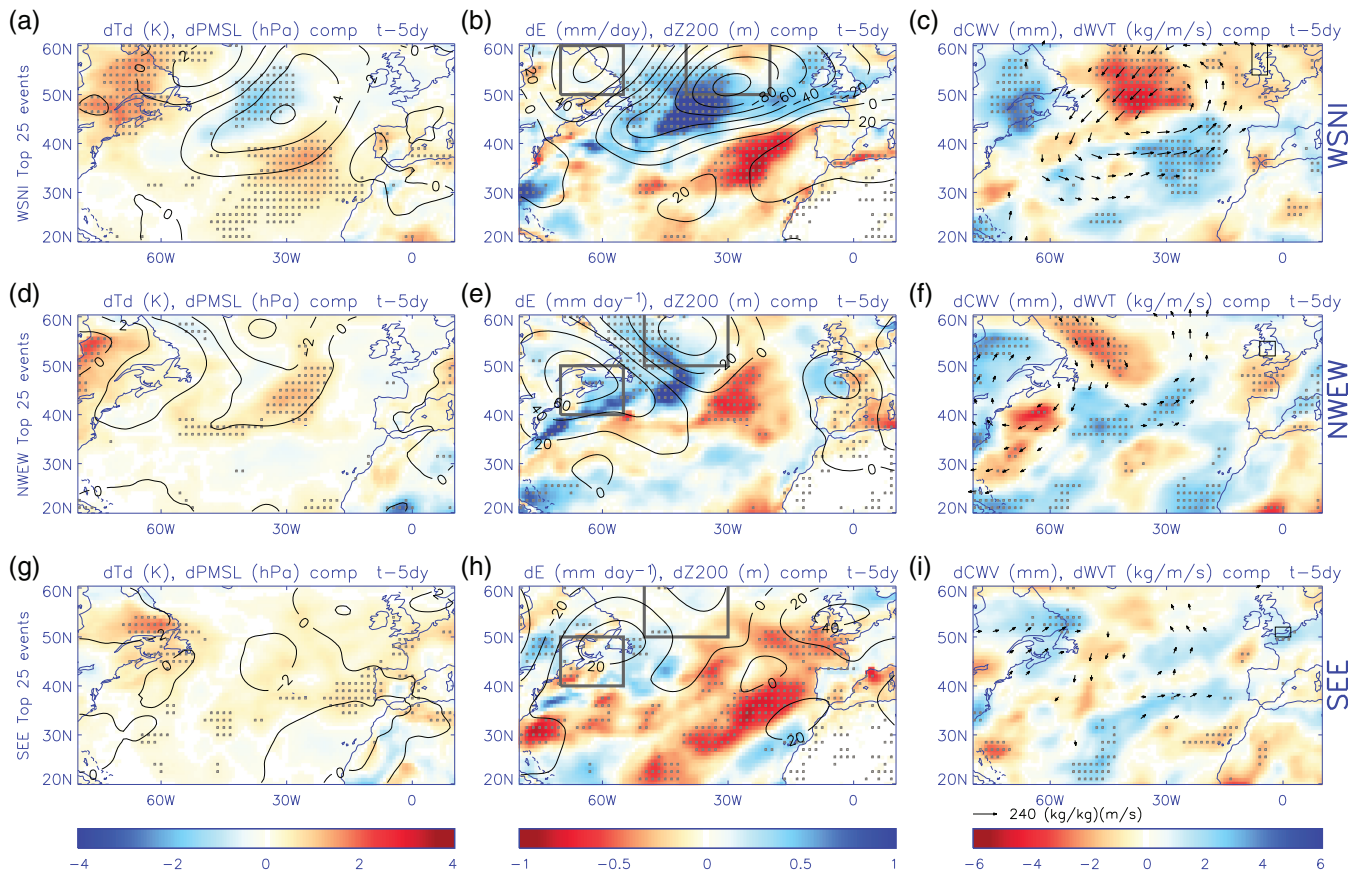
FIGURE 12 Large-scale atmospheric precursors to heaviest 25 rainfall events for WSNI (a–c), NWEW (d–f) and SEE (g–i). Boxes (b/e/h) show regions used to construct the geopotential height index, Z_I [Colour figure can be viewed at wileyonlinelibrary.com]

TABLE 2 Association between above 20th percentile Z_I anomalies (Z_I') and the heaviest 50 or 25 3-hourly rainfall events 5 and 9 days later for south East England (SEE), north West England and Wales (NWEW) and West Scotland and Northern Ireland (WSNI)

Region	Days prior	% top 50	% top 25	P(top 50)	P(top 25)
SEE	9	**28%**	**40%**	**2.1%**	**1.5%**
SEE	5	18%	**32%**	1.4%	**1.2%**
NWEW	9	**30%**	**48%**	**2.3%**	**1.8%**
NWEW	5	**36%**	**32%**	**2.7%**	**1.2%**
WSNI	9	**30%**	**40%**	**2.3%**	**1.5%**
WSNI	5	**40%**	**52%**	**3.0%**	**2.0%**
Chance	–	20%	20%	1.5%	0.7%
Maximum	–	100%	100%	7%	4%

Note: Columns 3–4 display the percentage of events preceded by elevated Z_I; columns 5–6 show the percentage of elevated Z_I days that precede the heaviest rainfall events. Association greater than chance are denoted with bold.

the SEE region (40% of the heaviest events were preceded by the highest 20% of Z_I and just 1.5% of high Z_I anomalies matched intense rainfall events 9 days later). For WSNI, a more coherent signal is present and over half of the heaviest 25 rainfall events correspond with the top 20% of Z_I anomalies 5 days prior and 3% of these elevated Z_I values match one of the heaviest 50 rainfall events 5 days later A more sophisticated statistical assessment, for example using bootstrapping, was not deemed worthwhile given the weak association identified in this case but could be considered if a more robust link was identified in the future. Given the apparent low skill, it was decided not to investigate this further, though a more detailed future assessment could potentially lead to improved physical understanding and predictability of the link between large-scale atmospheric patterns and precipitation extremes.

4 | CONCLUSIONS

Atmospheric precursors to the most intense 3-hourly summer rainfall events observed by gauges across the United Kingdom are constructed from the ERA-Interim reanalysis over the period 1979–2014. Work by Champion *et al.* (2019) is extended to consider all UK regions and additional thermodynamic variables, exploiting an updated quality controlled rainfall dataset and considering the Western Europe region at finer scales. Composites of atmospheric precursors are computed for the most extreme 25 and heaviest 200 rainfall events across each of six UK regions assessed.

In the day before the heaviest 200 summer rainfall events, negative anomalies in sea level pressure (around −2 to −6 hPa) and 200 hPa geopotential height (around −60 to −100 m) are identified to the west or south west of the United Kingdom. These coincide with above-average moisture, evaporation and dew point temperature over North West Europe. These signals emerge 4 days earlier, although the dynamical fields are less coherent for south east England events. Atmospheric precursors are found to be of larger magnitude and more diverse between regions for composites associated with the 25 heaviest rainfall events. They are characterized by a coherent increase in column integrated moisture locally of around 3–4 mm in 1 day, similar in magnitude but more rapid than for the 200 event composite. Geopotential height increases to the east of the United Kingdom 4 days prior to the most extreme 25 events for SEE and SWEW with average or below average moisture. This could indicate that drier, anticyclonic conditions, as suggested by weakly positive sea level pressure anomalies, could be necessary to generate the most extreme events. Reduced soil moisture availability arising from dry conditions alters the balance between the surface latent heat flux from evaporation and the sensible heat flux, resulting in warmer air temperatures and inducing modifications in the planetary boundary layer with potential impacts on convection. Interestingly, Blenkinsop *et al.* (2015) identified anticyclonic synoptic conditions as the only meteorological regime experiencing above-Clausius Clapeyron increases in hourly precipitation intensity with warmer temperatures for the United Kingdom.

The heaviest 25 sub-daily rainfall events affecting three regions of the United Kingdom (WSNI, NWEW, SEE) are associated with coherent atmospheric circulation patterns that emerge over the North Atlantic 5 days earlier. A tripole geopotential anomaly pattern across the North Atlantic is characterized by positive geopotential height anomalies over Newfoundland and to a lesser extent near to the United Kingdom with negative anomalies to the south of Greenland; these are only weakly associated with an increased chance of the heaviest rainfall events 5 days later. However, a strongly negative geopotantial height and sea level pressure anomaly are evident 5 days prior to the heaviest 25 events affecting west Scotland and Northern Ireland. Positive dew point temperature over Newfoundland and increased evaporation over the North Atlantic develop at this time and appear to propagate towards the United Kingdom although this is less marked for SEE events.

Heavy summer rainfall events are physically linked with anomalous geopotential heights that are symptomatic of a more disturbed, less zonal (west to east) jet stream that favours blocking of westerly flow. This results in enhanced or suppressed thunderstorm activity over Europe depending on the position of the atmospheric blocking pattern (Mohr *et al.*, 2019). Atmospheric blocking can cause heat to build up in regions dominated by high pressure, particularly where soils are dry and solar radiation primarily heats the ground rather than being used in evaporating surface water. Where warm, moist southerly flows are also induced this can supply the energy and moisture required for intense rainfall. Previous work has identified such a response over Southern France and Northern Italy following upper level disturbances that can often be triggered by remote Rossby waves (Nuissier *et al.*, 2011; Grazzini *et al.*, 2019). Thunderstorm activity, that can occasionally become organized mesoscale convective systems, is often enhanced during hot, moist and unstable southerly airflows, commonly referred to as Spanish Plumes when they influence the United Kingdom (Gray and Marshall, 1998).

As the climate warms, heavy rainfall is expected to intensify due to the greater amount of atmospheric moisture driven by the Clausius Clapeyron equation (Allan *et al.*, 2014; Dunn *et al.*, 2017). Changes in the dynamical characteristics of storms strongly modulate this simple expectation (Fischer and Knutti, 2016; Lenderink and Fowler, 2017) with intensification of individual storm systems due to enhanced latent heat release (Nie *et al.*, 2018). It is less clear how the frequency of meteorological events associated with heavy rainfall will alter as the planet warms since this is dependent upon complex dynamical effects and feedbacks involving land, ocean and ice (e.g., Coumou *et al.*, 2014; Dwyer and O'Gorman, 2017; Zappa *et al.*, 2018; Boers *et al.*, 2019). For example, spatial shifts in large-scale circulation patterns will strongly influence the frequency of synoptic conditions that favour extreme precipitation such as more anticyclonic conditions affecting the Southern United Kingdom (Chan *et al.*, 2016) or the frequency of hot, moist Spanish Plume events (Lewis and Gray, 2010). A more meandering jet stream in response to human-caused climate

change has been proposed (e.g., Francis and Vavrus, 2015; Mann *et al.*, 2017) and this could potentially increase the frequency of severe heatwaves as well as intense rainfall events affecting summer months (Kornhuber *et al.*, 2019). However the influence of tropical disturbances on mid-latitude extremes and how this connection evolves is also increasingly being appreciated (Wulff *et al.*, 2017; Scoccimarro *et al.*, 2018; Boers *et al.*, 2019). This underlines the importance of investigating how the atmospheric circulation alters in a warming planet. Yet a pragmatic and physically reasonable view is that while the United Kingdom will continue to experience fluctuations in weather patterns, when these conspire to produce heavy rainfall, these events will intensify with the possibility for more severe flooding when they occur. Exploiting information from the atmospheric precursor composites developed in this study can provide contextual information, potentially of benefit in forecasting flash flood situations (Flack *et al.*, 2019). It is also vital that observations are used to understand how rainfall is currently changing and it is imperative that reliability and homogeneity, inevitably impacting interpretation, continues to be improved.

ACKNOWLEDGEMENTS

ORCID

Richard P. Allan https://orcid.org/0000-0003-0264-9447

ENDNOTES

[1] Met Office Daily Weather Reports: https://digital.nmla.metoffice.gov.uk/

[2] https://www.ofcom.org.uk/__data/assets/pdf_file/0025/74356/mo_ofcom_report.pdf

REFERENCES

Ali, H., Fowler, H.J. and Mishra, V. (2018) Global observational evidence of strong linkage between dew point temperature and precipitation extremes. *Geophysical Research Letters*., 45(22), 12,320–12,330. https://doi.org/10.1029/2018GL080557.

Allan, R., Liu, C., Zahn, M., Lavers, D., Koukouvagias, E. and Bodas-Salcedo, A. (2014) Physically consistent responses of the global atmospheric hydrological cycle in models and observations. *Surveys in Geophysics*, 35, 533–552. https://doi.org/10.1007/s10712-012-9213-z.

Allan, R.P., Lavers, D.A. and Champion, A.J. (2015) Diagnosing links between atmospheric moisture and extreme daily precipitation over the UK. *International Journal of Climatology*, 36(9), 3191–3206. https://doi.org/10.1002/joc.4547.

Bao, J., Sherwood, S.C., Alexander, L.V. and Evans, J.P. (2017) Future increases in extreme precipitation exceed observed scaling rates. *Nature Climate Change*, 7(2), 128–132. https://doi.org/10.1038/nclimate3201.

Blenkinsop, S., Chan, S.C., Kendon, E.J., Roberts, N.M. and Fowler, H.J. (2015) Temperature influence on intense UK hourly precipitation and dependency on large-scale circulation. *Environmental Research Letters*, 10, 054021. https://doi.org/10.1088/1748-9326/10/5/054021.

Blenkinsop, S., Lewis, E., Chan, S.C. and Fowler, H.J. (2016) Quality-control of an hourly rainfall dataset and climatology of extremes for the UK. *International Journal of Climatology*, 37(2), 722–740. https://doi.org/10.1002/joc.4735.

Boers, N., Goswami, B., Rheinwalt, A., Bookhagen, B., Hoskins, B. and Kurths, J. (2019) Complex networks reveal global pattern of extreme-rainfall teleconnections. *Nature*, 566, 373–377. https://10.1038/s41586-018-0872-x

Carlson, T.N. and Ludlam, F.H. (1968) Conditions for the occurrence of severe local storms. *Tellus*, 20, 203–226. https://doi.org/10.1111/j.2153-3490.1968.tb00364.x.

Champion, A.J., Allan, R.P. and Lavers, D.A. (2015) Atmospheric rivers do not explain UKsummer extreme rainfall. *Journal of Geophysical Research: Atmospheres*, 120(14), 6731–6741. https://doi.org/10.1002/2014jd022863.

Champion, A.J., Blenkinsop, S., Li, X.-F. and Fowler, H.J. (2019) Synoptic-scale precursors of extreme U.K. summer 3-hourly rainfall. *Journal of Geophysical Research: Atmospheres*, 24, 4477–4489. https://doi.org/10.1029/2018jd029664.

Chan, S.C., Kendon, E.J., Roberts, N.M., Fowler, H.J. and Blenkinsop, S. (2016) The characteristics of summer sub-hourly rainfall over the southern UK in a high-resolution convective permitting model. *Environmental Research Letters*, 11(9), 94 024. https://doi.org/10.1088/1748-9326/11/9/094024.

Coumou, D., Petoukhov, V., Rahmstorf, S., Petri, S. and Schellnhuber, H.J. (2014) Quasi-resonant circulation regimes and hemispheric synchronization of extreme weather in boreal summer. *Proceedings of the National Academy of Sciences of the United States of America*, 111(34) 12331–12336. https://doi.org/10.1073/pnas.1412797111.

Dacre, H.F., Clark, P.A., Martinez-Alvarado, O., Stringer, M.A. and Lavers, D.A. (2014) How do atmospheric rivers form? *Bulletin of the American Meteorological Society*, 96, 1243–1255. https://doi.org/10.1175/bams-d-14-00031.1.

Dacre, H.F., Martínez-Alvarado, O. and Mbengue, C.O. (2019) Linking atmospheric rivers and warm conveyor belt airflows. *Journal of Hydrometeorology*, 20, 1183–1196. https://doi.org/10.1175/JHM-D-18-0175.1.

Darwish, M.M., Fowler, H.J., Blenkinsop, S. and Tye, M.R. (2018) A regional frequency analysis of UKsub-daily extreme precipitation and assessment of their seasonality. *International Journal of Climatology*, 38(13), 4758–4776. https://doi.org/10.1002/joc.5694.

Dee, D.P., et al. (2011) The ERA-interim reanalysis: configuration and performance of the data assimilation system. *Quarterly*

Journal of the Royal Meteorological Society, 137, 553–597. https://doi.org/10.1002/qj.828.

Dettinger, M.D., Ralph, F.M., Das, T., Neiman, P.J. and Cayan, D.R. (2011) Atmospheric rivers, floods and the water resources of California. *Water*, 3, 445–478. https://doi.org/10.3390/w3020445.

Dunn, R.J.H., Willett, K.M., Ciavarella, A. and Stott, P.A. (2017) Comparison of land surface humidity between observations and CMIP5 models. *Earth System Dynamics*, 8(3), 719–747. https://doi.org/10.5194/esd-8-719-2017.

Dwyer, J.G. and O'Gorman, P.A. (2017) Changing duration and spatial extent of midlatitude precipitation extremes across different climates. *Geophysical Research Letters*, 44(11), 5863–5871. https://doi.org/10.1002/2017GL072855.

Fischer, E.M. and Knutti, R. (2016) Observed heavy precipitation increase confirms theory and early models. *Nature Climate Change*, 6(11), 986–991. https://doi.org/10.1038/nclimate3110.

Flack, D., et al. (2019) Recommendations for improving integration in national end-to-end flood forecasting systems: an overview of the FFIR (flooding from intense rainfall) programme. *Water*, 11(4), 725. https://doi.org/10.3390/w11040725.

Francis, J. A. and S. J. Vavrus, 2015: Evidence for a wavier jet stream in response to rapid arctic warming. *Environmental Research Letters*, 10 (1), 014 005, doi: https://doi.org/10.1088/1748-9326/10/1/014005.

Gimeno, L., Nieto, R., Vazquez, M. and Lavers, D.A. (2014) Atmospheric rivers: a mini-review. *Frontiers in Earth Science*, 2. https://doi.org/10.3389/feart.2014.00002.

Golding, B., Clark, P. and May, B. (2005) The boscastle flood: meteorological analysis of the conditions leading to flooding on august 16, 2004. *Weather*, 60, 230–235. https://doi.org/10.1256/wea.71.05.

Gray, M.E.B. and Marshall, C. (1998) Mesoscale convective systems over the UK, 1981-97. *Weather*, 53(11), 388–396. https://doi.org/10.1002/j.1477-8696.1998.tb06352.x.

Grazzini, F., Craig, G.C., Keil, C., Antolini, G. and Pavan, V. (2019) Extreme precipitation events over northern italy. part i: A systematic classification with machine-learning techniques. *Quarterly Journal of the Royal Meteorological Society*, in press. https://doi.org/10.1002/qj.3635.

Guerreiro, S.B., Fowler, H.J., Barbero, R., Westra, S., Lenderink, G., Blenkinsop, S., Lewis, E. and Li, X.-F. (2018) Detection of continental-scale intensification of hourly rainfall extremes. *Nature Climate Change*, 8(9), 803–807. http://doi.org/10.1038/s41558-018-0245-3.

Hapuarachchi, H.A.P., Wang, Q.J. and Pagano, T.C. (2011) A review of advances in flash flood forecasting. *Hydrological Processes*, 25(18), 2771–2784. https://doi.org/10.1002/hyp.8040.

Institute of Hydrology. *Hydrological data United Kingdom 1995 Yearbook: an account of rainfall, river flows, groundwater levels and river water quality January to December 1995*; 1996. Hydrological data UK, Vol. 1995.

Jones, M.R., Blenkinsop, S., Fowler, H.J. and Kilsby, C.G. (2013) Objective classification of extreme rainfall regions for the UKand updated estimates of trends in regional extreme rainfall. *International Journal of Climatology*, 34(3), 751–765. https://doi.org/10.1002/joc.3720.

Kendon, E.J., Roberts, N.M., Fowler, H.J., Roberts, M.J., Chan, S.C. and Senior, C.A. (2014) Heavier summer downpours with climate change revealed by weather forecast resolution model. *Nature Climate Change*, 4(7), 570–576. https://doi.org/10.1038/nclimate2258.

Kornhuber, K., Osprey, S., Coumou, D., Petri, S., Petoukhov, V., Rahmstorf, S. and Gray, L. (2019) Extreme weather events in early summer 2018 connected by a recurrent hemispheric wave-7 pattern. *Environmental Research Letters*, 14(5) 054 002. https://doi.org/10.1088/1748-9326/ab13bf.

Lavers, D.A., Allan, R.P., Wood, E.F., Villarini, G., Brayshaw, D.J. and Wade, A.J. (2011) Winter floods in Britain are connected to atmospheric rivers. *Geophysical Research Letters*, 38, L23803. https://doi.org/10.1029/2011GL049783.

Lavers, D.A., Hannah, D.M. and Bradley, C. (2015) Connecting large-scale atmospheric circulation, river flow and groundwater levels in a chalk catchment in southern England. *Journal of Hydrology*, 523, 179–189. https://doi.org/10.1016/j.jhydrol.2015.01.060.

Lavers, D.A., Pappenberger, F., Richardson, D.S. and Zsoter, E. (2016) ECMWF extreme forecast index for water vapor transport: a forecast tool for atmospheric rivers and extreme precipitation. *Geophysical Research Letters*, 43(22), 11,852–11,858. https://doi.org/10.1002/2016gl071320.

Lenderink, G. and Fowler, H.J. (2017) Understanding rainfall extremes. *Nature Climate Change*, 7(6), 391–393. https://doi.org/10.1038/nclimate3305.

Lenderink, G. and van Meijgaard, E. (2010) Linking increases in hourly precipitation extremes to atmospheric temperature and moisture changes. *Environmental Research Letters*, 5, 025208. https://doi.org/10.1088/1748-9326/5/2/025208.

Lewis, E., et al. (2018) A rule based quality control method for hourly rainfall data and a 1km resolution gridded hourly rainfall dataset for Great Britain: CEH-GEAR1hr. *Journal of Hydrology*, 564, 930–943. https://doi.org/10.1016/j.jhydrol.2018.07.034.

Lewis, M.W. and Gray, S.L. (2010) Categorisation of synoptic environments associated with mesoscale convective systems over the UK. *Atmospheric Research*, 97, 194–213. https://doi.org/10.1016/j.atmosres.2010.04.001.

Mann, M.E., Rahmstorf, S., Kornhuber, K., Steinman, B.A., Miller, S.K. and Coumou, D. (2017) Influence of anthropogenic climate change on planetary wave resonance and extreme weather events. *Scientific Reports*, 7(45), 242. https://doi.org/10.1038/srep45242.

McGinnigle, J.B. (2002) The 1952 Lynmouth floods revisited. *Weather*, 57, 235–242. https://doi.org/10.1256/004316502760195894.

Mohr, S., Wandel, J., Lenggenhager, S. and Martius, O. (2019) Relationship between atmospheric blocking and warm season thunderstorms over western and central europe. *Quarterly Journal of the Royal Meteorological Society*. 145, 3040–3056. https://doi.org/10.1002/qj.3603.

Nie, J., Sobel, A.H., Shaevitz, D.A. and Wang, S. (2018) Dynamic amplification of extreme precipitation sensitivity. *Proceedings of the National Academy of Sciences*, 115(38) 9467–9472. https://doi.org/10.1073/pnas.1800357115.

Nuissier, O., Joly, B., Joly, A., Ducrocq, V. and Arbogast, P. (2011) A statistical downscaling to identify the large-scale circulation patterns associated with heavy precipitation events over

southern France. *Quarterly Journal of the Royal Meteorological Society*, 137(660), 1812–1827. https://doi.org/10.1002/qj.866.

O'Gorman, P. A., 2015: Precipitation extremes under climate change. *Current Climate Change Reports*, 1 (2), 49–59, https://doi.org/10.1007/s40641-015-0009-3.

Pendergrass, A.G. (2018) What precipitation is extreme? *Science*, 360(6393), 1072–1073. http://doi.org/10.1126/science.aat1871.

Pendergrass, A.G., Reed, K.A. and Medeiros, B. (2016) The link between extreme precipitation and convective organization in a warming climate: global radiative-convective equilibrium simulations. *Geophysical Research Letters*, 43(21), 11,445–11,452. https://doi.org/10.1002/2016GL071285.

Pfahl, S., O'Gorman, P.A., Fischer, E.M., O'Gorman, P.A., Fischer, E.M., O'Gorman, P.A. and Fischer, E.M. (2017) Understanding the regional pattern of projected future changes in extreme precipitation. *Nature Climate Change*, 7(6), 423–427. https://doi.org/10.1038/nclimate3287.

Scoccimarro, E., Gualdi, S. and Krichak, S. (2018) Extreme precipitation events over North-Western Europe: getting water from the tropics. *Annals of Geophysics*, 61, p. OC449. https://doi.org/10.4401/ag-7772.

Smith, K. and Ward, R. (1998) *Floods: Physical Processes and Human Impacts*. Chichester, UK: Wiley. ISBN: 978-0-471-95248-0.

Stephens, E., Day, J.J., Pappenberger, F. and Cloke, H. (2015) Precipitation and floodiness. *Geophysical Research Letters*, 42(23), 10 316–10 323. https://doi.org/10.1002/2015GL066779.

Wasko, C. and Sharma, A. (2017) Global assessment of flood and storm extremes with increased temperatures. *Scientific Reports*, 7(1), 7945. https://doi.org/10.1038/s41598-017-08481-1.

Wulff, C.O., Greatbatch, R.J., Domeisen, D.I.V., Gollan, G. and Hansen, F. (2017) Tropical forcing of the summer East Atlantic pattern. *Geophysical Research Letters*, 44(21), 11,166–11,173. https://doi.org/10.1002/2017GL075493.

Zappa, G., Pithan, F. and Shepherd, T.G. (2018) Multimodel evidence for an atmospheric circulation response to Arctic Sea ice loss in the CMIP5 future projections. *Geophysical Research Letters*, 45(2), 1011–1019. https://doi.org/10.1002/2017GL076096.